POLITECNICO DI TORINO
Repository ISTITUZIONALE

First results from microseismic monitoring of a rockslide at Madonna del Sasso (Verbania, Italy)

Publisher copyright

(Article begins on next page)

04 August 2020

GRUPPO NAZIONALE DI GEOFISICA DELLA TERRA SOLIDA

Atti del
33° Convegno Nazionale

Tema 3: Geofisica applicata

Bologna, 25-27 novembre 2014
Palazzo della Regione

FIRST RESULTS FROM MICROSEISMIC MONITORING OF A ROCKSLIDE AT MADONNA DEL SASSO (VERBANIA, ITALY)

C. Colombero[1], C. Comina[1], A. Fiaschi[2], G. Saccorotti[3], S. Vinciguerra[1,4,5]
[1] Dipartimento di Scienze della Terra, Università degli Studi di Torino, Italy
[2] Fondazione Prato Ricerche, Prato, Italy
[3] Istituto Nazionale di Geofisica e Vulcanologia, Pisa, Italy
[4] Department of Geology, University of Leicester, Leicester, UK
[5] British Geological Survey, UK

Introduction. The hazard mitigation of rockslides and the understanding of their time evolution are a main task particularly when a pre-existing fracture system affects the rock mass. Instability can rapidly accelerate to failure without clear precursory warnings. Traditional monitoring techniques (inclinometers, tiltmeters, extensometers, ...) may be inadequate to forecast the dynamics of evolution and provide quantitative elements for the development of an early warning system. Since a persistent fracture system originates from the genesis, growth and progressive coalescence of microcracks, it is key to constrain the initial stages of rupture. The energy release, in the form of elastic waves, associated with the formation of microcracks can be detected by a microseismic monitoring network. The location of the microseismic events and the monitoring of their time and spatial evolution with particular reference to potential destabilizing factors, such as rainfalls and temperature changes, can provide information with respect to the understanding of the unstable sectors within the rock mass and the prediction of the possible acceleration to the failure.

To understand the failure processes and to search for precursory patterns to failure, the microseismic technique has been extensively used in rock samples at the laboratory scale and at intermediate scales in quarries, mines or tunnels. Conversely, only a few applications exist at the landslides/rockslides scale, and thus it is a priority testing the ability of microseismic monitoring in giving interesting insights into gravitational instability and, in very few cases, in providing precursory patterns for failure forecasting and hazard assessments. Interesting applications on unstable rock slopes and rockfalls have been developed by Spillman *et al.* (2007), Amitrano *et al.* (2010), Helmstetter and Garambois (2010) and Levy *et al.* (2011), studies on rocky cliff instabilities (Amitrano *et al.*, 2005) and mudslides (Amitrano *et al.*, 2007) are also reported.

In this paper we present the first results from a microseismic monitoring network installed at Madonna del Sasso (NW Italy) to monitor rock instability phenomenon highlighted by neat and long lasting episodes of slow deformation recorded by standard monitoring devices (topographic measurements, borehole inclinometers, crackmeters and extensometers).

A detailed geophysical and geomechanical characterization of the site has been preliminarily undertaken in order to define the overall geometry and the fracturing state of the instable rock mass and to establish the best position of the nodes for the monitoring network. Furthermore the definition of the seismic velocity field inside the rock mass is a fundamental parameter for the processing of the recorded microseismic signals, in order to localize the microseismic events. We also analyzed the signals acquired during the first six months of monitoring. We present the first results, and we aim to develop objective and automatic procedures for signal classification and event localization.

The test site. The cliff of Madonna del Sasso (45° 79' N, 8° 37' E) is located in NW Italy, on the western shore of the Orta Lake. It is a high massive granite outcrop bordered on three sides (N, E and S) by roughly vertical walls, with a height of about 200 m (Fig. 1a). The top of the relief is located at an altitude of approximately 650 m a.s.l. and it is occupied by a panoramic square, in front of the XVIII-century sanctuary from which the place takes its name.

From a geological point of view, the area is totally characterized by a granitic rock mass, known as Granito di Alzo. The actual morphology has been heavily affected from intense mining activity carried out until a few decades ago. A preliminary geomechanical characterization
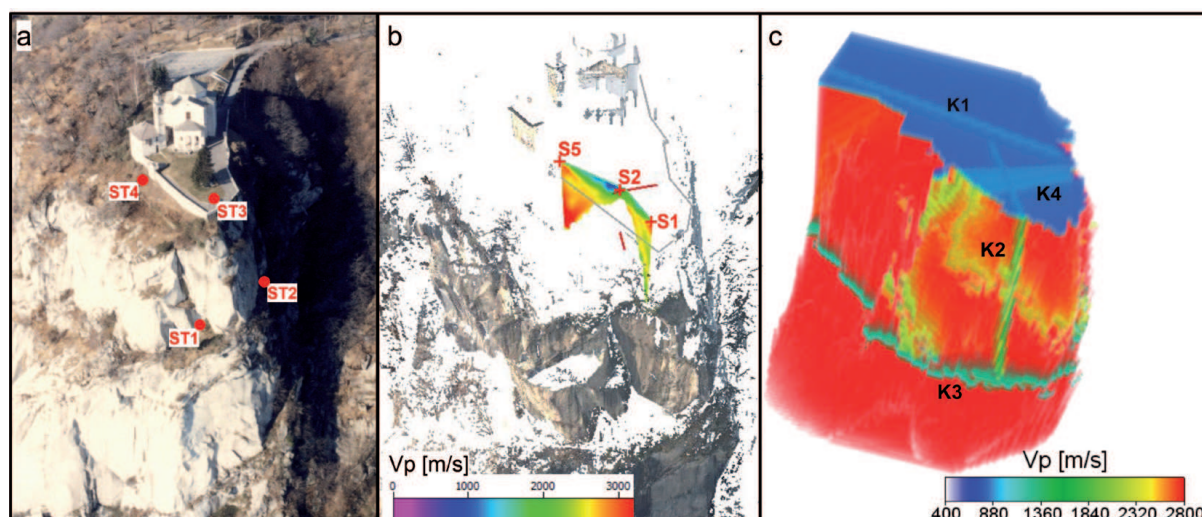
Fig. 1 – Building of a 3-D seismic velocity model for microseismic event localization. a) The cliff of Madonna del Sasso (NW Italy) with the location of the four triaxial geophones of the monitoring network. b) The point cloud obtained from a previous laser-scanner survey with the results of the cross-hole seismic tomography between the inclinometric boreholes S1, S2 and S5. c) Rendering of the 3-D velocity model for P waves obtained from DSM, cross-hole tomography results, geological and geomechanical observations and measurements.

(Lancellotta *et al.*, 1991) led to the identification of four main joint sets (dip direction/dip): K1 (110/75), K2 (0/80), K3 (150/15) and K4 (50/75). These discontinuities tend to isolate the north-western frontal portion of the cliff which increases its instability as a function of the rock joints along the fractures and its foot edge. A volume of about 12,000 m^3 has been estimated forming the instable sector. Particularly along a K4 discontinuity there is a clear evidence of movement: a decimetric step dislocates the lawn and the confining walls of the panoramic square.

Geophysical investigation. Focusing on the gravitative processes that affect the studied rock mass, a good knowledge of the fracturing state is an important requirement for the stability analysis, with particular reference to orientation, spacing, opening and persistence, filling and hydraulic conditions of the discontinuities. With this aim, we extended a previous cross-hole seismic tomography (Colombero and Comina, 2014) realized in the yard in front of the sanctuary, in order to obtain a tomographic image between three available inclinometric boreholes (Fig. 1b). To perform the tests a Borehole Impacter Source by Geotomographie GmbH was used as in-hole source in the S2 borehole, with three different locations till a depth of about 6 m (after this depth an obstruction of the hole casing inhibited deeper measurements) while a sledge hammer, impinging both vertically and horizontally on a steel rod, was employed as surface source in different locations along the lines connecting the three holes.

A prototype borehole string equipped with 8 three-component geophones (10 Hz) at 1 m spacing, stiffly connected by a PVC bar that permits to control geophone orientation, was progressively lowered (with a 2-geophone superposition each subsequent positioning) in the S1 and S5 soundings, till the maximum available depth (respectively of 27 and 21 m). On the lawn surface 4 three-component geophones (2 Hz) were placed along the lines connecting the three boreholes, with a reciprocal spacing of 2.5 m (along S1-S2) and 4 m (along S2-S5).

First break manual picking was performed on the acquired seismic traces, on the pertaining components, to allow for both P- and S-wave velocities imaging. Data were inverted to obtain a tomographic image between the investigated volume with the use of GeoTomCG software, which performs three-dimensional tomographic analysis with source and receiver positions in any configuration within a 3-D grid. The software allows for curved-ray calculations which have been observed to be more accurate in case of strong velocity contrasts. Curved ray tracing is performed with a revised form of ray bending, derived from the Um and Thurber (1987)

method. Inversions are performed with the simultaneous iterative reconstruction technique (SIRT, Lytle *et al.*, 1978; Peterson *et al.*, 1985).

Given the test disposition (reduced ray coverage due to difficulties in lowering the in-hole source) and the hole casing (possible interference of tube waves) the resulting seismic sections have to be considered with particular precautions. Nevertheless in both seismic sections (an example for P wave is reported in Fig. 1b) a shallow coverage of low velocity materials of about 2 m (top soil and highly altered/fractured granite, as also resulting from S1 and S2 core logs) is evidenced. A clear refraction boundary is noticed below this zone revealing an interface with a high-velocity but non-homogeneous formation. Intact granite velocity reaches about 2.9-3.1 km/s for P waves and 1.6-1.8 km/s for S waves. Estimated velocities appear to be quite low for an intact granite formation; direct measurement on rock samples are planned in this respect to obtain a direct verification. Two main low-velocity zones (about 2.2-2.4 km/s for P waves and 1.2-1.4 km/s for S waves) are also evidenced in both seismic sections within the massive granite formation. The position and dip of these zones agree with the fractures of the K4 system (50/75) whose traces are directly visible on the yard in front of the sanctuary. Low seismic velocities depths quite well compare with the outcomes of the stratigraphic log along the S1 sounding, enabling to associate the reduction in velocity values to zones of the rock mass with clear evidence of recrystallized fractures and fractures with alteration patinas. Given the accordance of all these evidences, the geophysical survey reveals a non-uniform (in shape, opening and velocity values) sliding plane probably associated with the presence of rock bridges whose ruptures could be the main cause of instability and which are the subject on which we focus the microseismic monitoring campaign.

The microseismic monitoring network. The microseismic network has been installed at Madonna del Sasso in November 2013. It consists of four triaxial geophones (4.5 Hz) connected to a multichannel acquisition system (Granite - Kinemetrics, Inc.). Geophone location is reported in Figure 1a. The first two geophones are placed on sheltered areas of the high walls of the cliff, at a height of about 50 m below the top yard, on the south-eastern (ST1) and northern (ST2) side of the instable volume. The other two stations are placed in shallow manholes accessible from the panoramic square: ST3 is located in the lawn, near the inclinometric borehole S1, and ST4 is outside this unstable area, SE from the sanctuary.

In the first operative weeks we managed to set up the best acquisition parameters for signal recording. We used a continuous recording at 250 Hz sampling frequency (later changed to 1 kHz in March 2014 for improving the first arrival time picking and obtain wider frequency content information) and a trigger recording based on a STA/LTA (Short Time Average over Long Time Average) detection algorithm.

The STA/LTA ratio is continuously calculated and if it exceeds the user defined STA/LTA trigger threshold level, for any channel of the monitoring network, trigger is declared on the whole network. The network de-triggers if the STA/LTA ratio falls below another preset value (STA/LTA de-trigger threshold level). All calculations are made for every data sample in each of the twelve channels connected to the recorder, ensuring minimal time delay between the microseismic event and the triggering. Since these parameters of seismological interest are mainly used for the detection of earthquakes, we made several attempts to find threshold values suitable for the microseismic monitoring. We set a small STA window duration (0.3 s) since the shorter it is, the more sensitive to short and high frequency signals the STA/LTA trigger should be, and a LTA window duration of 30 s, with a STA/LTA Trigger Threshold Level of 6. We also set a low value of STA/LTA de-trigger threshold (10%) to preserve complete coda waves for further analysis.

Each channel was assigned a number of votes that it may cast towards getting the system to trigger. We selected the number of votes each channel would contribute (when it is triggered) to the total number of votes required to trigger the system (12). We gave zero votes to the six channels of ST3 and ST4 that we didn't want to affect the triggering since they are located in

shallow manholes, easily influenced by human presence and activity on the square. We assigned 3 votes to all the other channels.

During November 2013 - March 2014 we recorded more than 2000 events with different waveforms, duration and frequency content. Our first aim is therefore to analyze and classify these signals and to extract only the ones with a possible relation with fracture processes. Their localization and time evolution can give important information in respect to the most active zones in the rock mass and their progression to failure.

First results of signal analysis and classification. The identification and classification of the recorded seismic signals is a major task for the monitoring of the stability at Madonna del Sasso. Each type of signal is related to different source processes, among which we would like to focus on those related to fracturing processes. Only after this classification the spatial localization and temporal distribution of the microseismic events could be used as an objective element to realize an early warning system. In order to achieve this goal, the classification of the recorded events should be done as close to real time as possible, with automatic procedures of analysis and classification of data. For these reasons, researches are involved in the development of automatic robust seismic event discrimination algorithms, enabling to reduce subjectivity and time of analysis and to concentrate only on a reduced number of signals.

Many efforts have been made in past years for the automatic recognition of seismo-volcanic events: the recent trend is to complement the human work with automatic recognition systems providing support in early warning (Aspinall *et al.*, 2006) or continuous volcano monitoring (Cortés *et al.*, 2009) scenarios. Several authors have successfully applied Hidden Markov Models (HMMs) to continuous volcano-seismic event recognition (Benítez *et al.*, 2007; Beyreuther *et al.*, 2008) rivalling in popularity with other techniques such as Artificial Neuronal Networks (ANNs) (Falsaperla *et al.*, 1996; Scarpetta *et al.*, 2005) and Support Vector Machines (SVMs) (Masotti *et al.*, 2006; Giacco *et al.*, 2009).

We are currently analysing manually the recorded events and characterizing them in time and frequency domains (Fig. 2), in order to identify the key parameters on which make reliable distinctions among the nature of each signal and to devise an automatic classification procedure. The considered parameters are signal shape (in terms of amplitude, duration, kurtosis) and frequency content (range of maximum frequency content, frequency distribution in spectrograms). Particularly the kurtosis of the envelope was found to be a crucial parameter for the description of a signal shape (Hilbert *et al.*, 2014). Kurtosis parameter (k) is a quantitative measurement of the flatness or peakedness of a random-variable distribution compared to a normal distribution. For a random variable, it can be expressed as the ratio between the fourth central moment and the fourth power of the standard deviation of the expected distribution:

$$k = \frac{E(x-\mu)^4}{\sigma^4} \tag{1}$$

where μ is the mean of x, σ is the standard deviation of x and $E(y)$ represents the expected value of the quantity y. In this way the kurtosis of a normal distribution is 3. Distributions that are flatter than normal have kurtosis values lower than three, sharper-distribution kurtosis is higher than 3.

As a first result, we can clearly distinguish four main classes of recorded signals: microseismic events, regional earthquakes, electrical noises and calibration signals, still unclassified events (probably grouping rockfalls, quarry blasts, other anthropic and natural sources of seismic noise).

Microseismic events (Fig. 2a) show impulsive and short duration signals which envelope has a triangle shape with a clear coda. The spectrogram has a specific aspect with a sharp energy increase followed by an exponential decay of the high-frequency content with time. These features are in good agreement with those reported by several authors (Burlini *et al.*, 2007; Helmstetter and Garambois, 2010; Levy *et al.*, 2011). As a result, they show very short duration (0.8-4 s) and very high kurtosis values (>10). Unlike the high frequency content expected for
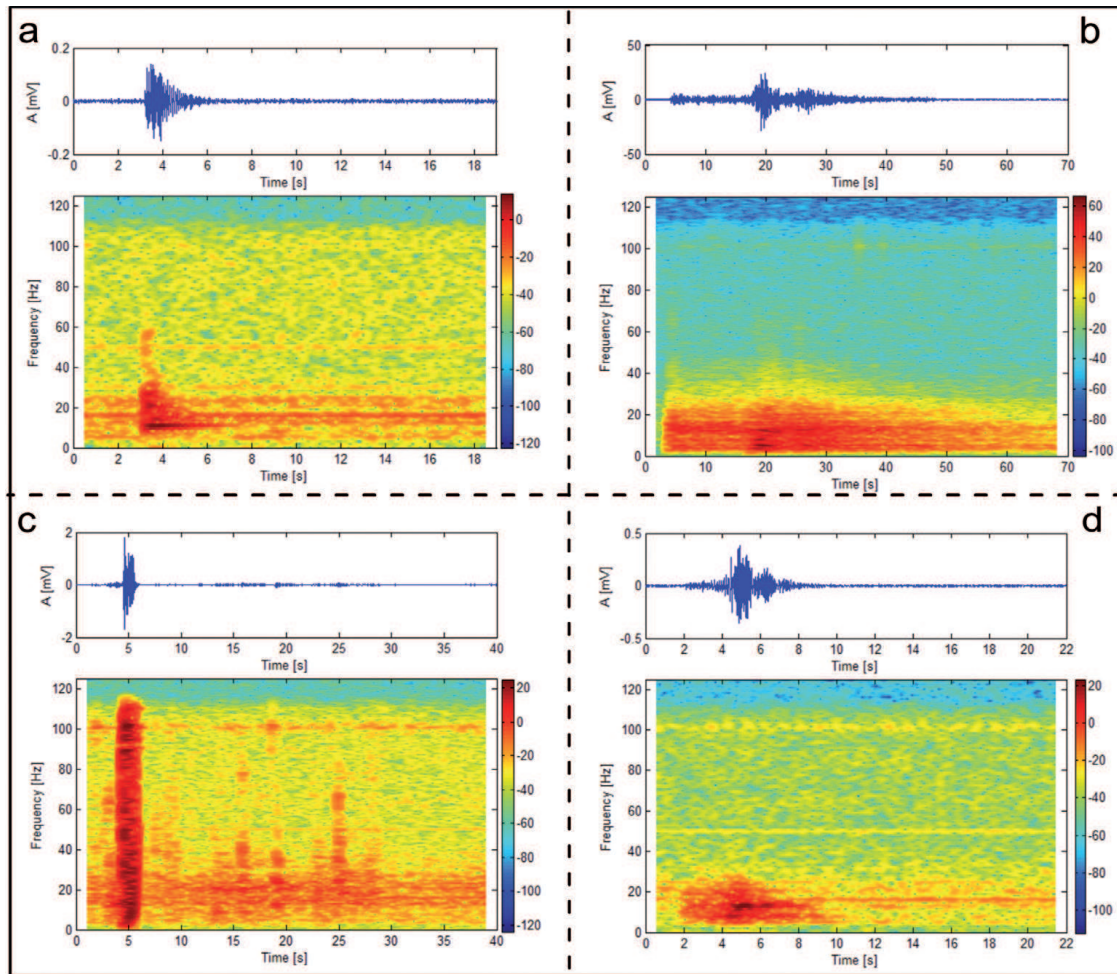
Fig. 2 – First classification of different types of signal: a) a microseismic event; b) an earthquake (Northern Italy, M_L=3.8, 2013-11-21 10:36:49.0 UTC, 44.91N 9.03E); c) electrical transient and d) still unclassified events.

this kind of signals, the ones recorded at Madonna del Sasso have the highest frequency content in the band 20-30 Hz. The lower frequency may be related to bigger source dimension, since it is known that the frequency content of the signal emitted by the fracture mechanism is a scale-dependent parameter (Amitrano *et al.*, 2010). On a series of 5-month monitoring data (over 2000 events) only 93 signals show these features (~4.5%).

Regional earthquakes (Fig. 2b) show lemon-shape envelope and long duration (30-60 s). Most of them are characterized by quite well separated impulsive P- and S-wave onsets. Their kurtosis values are always lower than 10. The maximum energy content is in the frequency range between 1 and 20 Hz, depending on the epicentral distance. Comparing the date and time of earthquake national and international catalogues, we surely identify 25 signals relative to this source mechanism.

Noise transients generated by electrical disturbances (Fig. 2c) are impulsive spike-like signals, with very short duration and high energy content (50-100 Hz). They are probably caused by atmospheric electrical discharges and other electrical disturbances due to the length of the connecting cables between the stations and the acquisition instrument, according with what observed by Spillman *et al.* (2007). Not by chance, most of this type of signals affect only ST1 and, in smaller amounts, ST2 which are located on the cliff walls with connection cables of more than 50-meters length. A high number of these signals was detected (~100).

At the present stage of this study, we grouped all the other events in an unclassified class (Fig. 2d). It may include rockfalls, quarry blasts and other sources of natural or anthropic
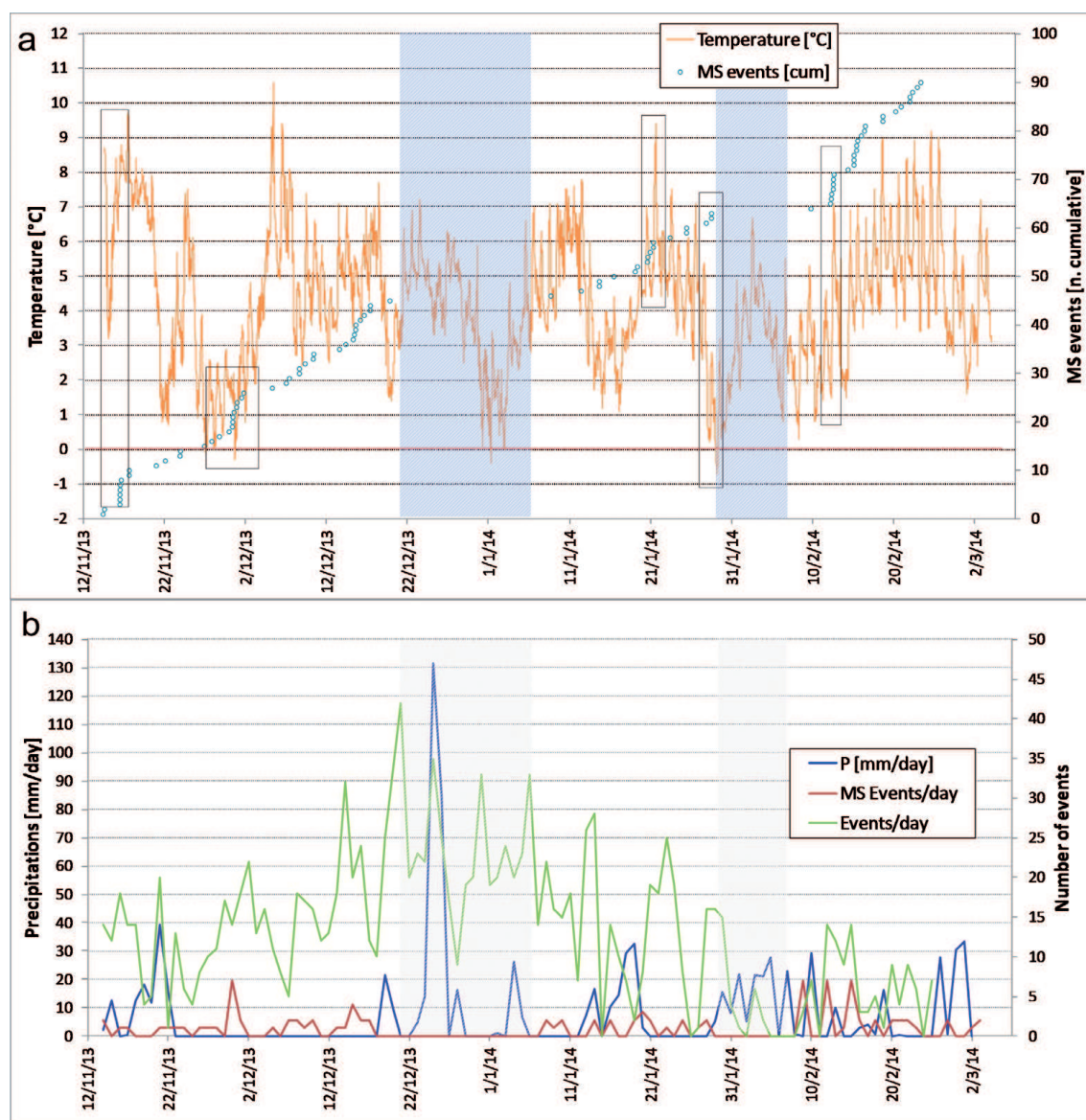
45

Fig. 3 – First comparisons between event rate and meteorological data for the period November 2013 - February 2014. (a) Temperature recorded by a probe on the southern cliff of Madonna del Sasso and probable microseismic event cumulative curve. Black rectangles point out the steeper parts of the cumulative curve in agreement with abrupt temperature changes. (b) Daily rainfalls measured at the Arpa Piemonte station of Cesara (VB) compared with the daily total number of events and the daily number of probable microseismic events. The coloured rectangles overlap periods in which signal recording was lacking and only event count was available.

disturbances. As we want to focus the study on microseismic events related to fracture processes we temporarily don't deepen the distinction and the research of their specific source mechanisms.

The comparison between event rate and meteorological data can give further information about microseismic source mechanisms and related temporal distribution. The correlation between temperature recorded by an automatic data logger placed on the southern cliff of Madonna del Sasso and the cumulative curve of probable microseismic events is shown in Fig. 3a. At a first sight a relationship between sudden accelerations in the number of microseismic events and abrupt changes (negative or positive) in the air temperature values can be observed. The largest number of probable microseismic events in a day (7) was recorded on 30 November 2013, when temperatures rapidly decreased under 0°C.

Unfortunately, in other periods of winter frost the monitoring network was not correctly working. Conversely rainfalls (obtained from a near monitoring station of ARPA Piemonte) seem not to affect the rate of probable microseismic events. However, it is somehow appreciable in Fig. 3b that rainfalls affect the total number of recordings. Water flow and seepage, entrainment of debris in the fracture zones near the geophones can trigger the system to record a larger number of events.

3-D velocity model. After identifying microseismic signals among the large and various number of recordings we located them within the rock mass to constrain the most unstable zones subjected to fractures and understand the evolution related to source position identification along a fracture zone.

At the current state, determining the hypocenter locations has been really challenging for several reasons: many channel recordings are very noisy and first arrival time picks are either lacking or inaccurate for some stations; even if we are monitoring a small volume, the seismic velocity inside the rock mass is highly heterogeneous, as it resulted from the geophysical characterization; there is no evidence of separated p and s onsets in the signals.

To try to overcome the problem we have built a three-dimensional P-wave velocity model joining the DSM (Digital Surface Model) of the cliff obtained from a laser-scanner survey, the results of the cross-hole seismic tomography, the geological observations and the geomechanical measures of the most pervasive fracture planes (Fig. 1c). To do this the original DSM point cloud has been cleaned from vegetation and man-made structures, to obtain a rough DTM (Digital Terrain Model) of the granite cliff. The point cloud has been then resampled to a geometric cubic grid of points at 0.5 m spacing. The air velocity (338 m/s) was assigned to the points having an elevation higher than the DTM, and a constant velocity to the intact granitic rock mass (the higher velocity found from cross-hole tomography). With a GPS measurement survey, we then accurately georeferenced the geophysical test lines and the major fracture traces directly accessible from the yard. We extrapolated in depth the trend of the discontinuities either from the tomographic inversion (for the K4 system) or from the mean dip and dip direction of the systems. The equation of the planes that best fitted these points located on the discontinuities has been found and we gave to those surfaces the lower velocity obtained from cross-hole tomography.

Now we have a quite accurate 3-D velocity model to be used for event localization (Fig. 1c). Tests with known seismic sources in accessible locations above the cliff are also planned in order to obtain a further direct verification of the used seismic velocities. Accordingly, to estimate the hypocenters of the microseismic events we will try to use the NonLinLoc (Non-Linear Location) software package of Lomax *et al.* (2000) for probabilistic, global-search earthquake location in 3D media.

Conclusions. This paper shows the first results of an ongoing work concerning the geophysical characterization of an instable rock mass and the signals acquired from the microseismic monitoring network.
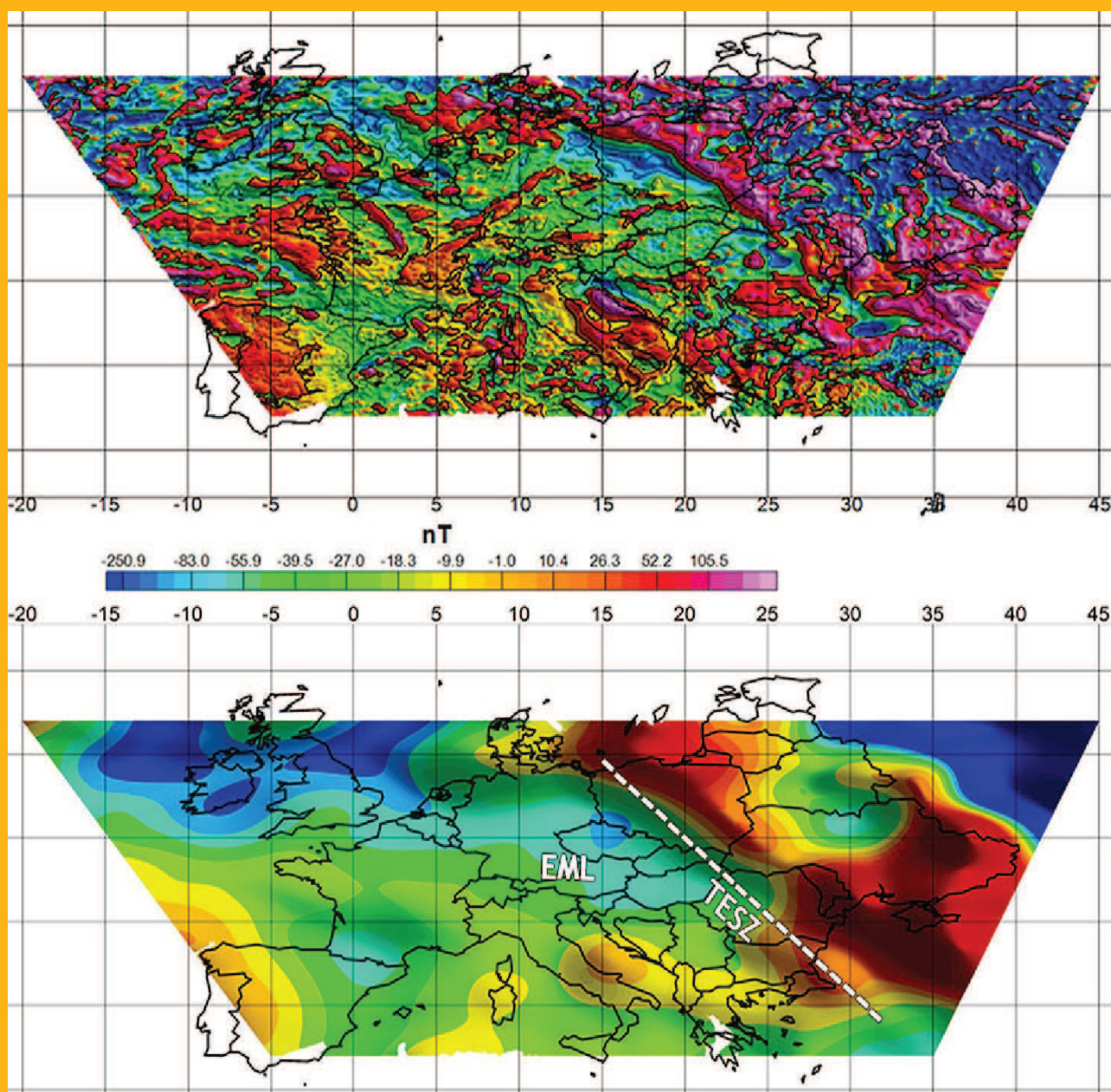
The seismic survey allowed investigating in depth the fracturing state of the granite mass, in order to better understand the instability mechanism and to design the monitoring system. The outcomes allowed us to better investigate the presence and geometry of discontinuities, revealing a non-uniform sliding plane, with associated heterogeneous P and S-wave velocities, probably suggesting the presence of rock bridges whose ruptures could be the main cause of instability and can be monitored by the monitoring network. The obtained 3-D velocity model is the basic requirement for the processing and location of the microseismic signals. From the observation of the first months of monitoring data, first steps towards an adequate signal analysis and classification have been made obtaining a preliminary classification of recorded events.

In the near future we will proceed to the localization of event sources, to the improvement and automation of data analysis procedures and to search for correlations between event rates and meteorological data, for a better global understanding of rock mass instability phenomena.

References

Amitrano D., Grasso J.R. and Senfaute G.; 2005: *Seismic precursory patterns before a cliff collapse and critical-point phenomena*. Geoph. Res. Let., **32** (8), L08314, doi:10.1029/2004GL022270.

Amitrano D., Gaffet S., Malet J.-P. and Maquaire O.; 2007: *Understanding mudslides through micro-seismic monitoring: The Super-Sauze (South French Alps) case study*. B. Soc. Geol. Fr., **178** (2), 149-157, doi:10.2113/gssgfbull.178.2.149.

Amitrano D., Arattano M., Chiarle M., Mortara G., Occhiena C., Pirulli M. and Scavia C.; 2010: *Microseismic activity analysis for the study of the rupture mechanisms in unstable rock masses*, Nat. Hazards Earth Syst. Sci., **10** (4), 831-841.

Aspinall W., Carniel R., Jaquet O., Woo G. and Hincks T.; 2006: *Using hidden-multistate Markov models with multi-parameter volcanic data to provide empirical evidence for alert level decision-support*. Journal of Volcanology and Geothermal Research, **153** (1), 112–124.

Benítez C., Ramírez J., Segura J.C., Ibáñez J., Almendros J., García-Yeguas A. and Cortés G.; 2007: *Continuous HMM-based seismic-event classification at Deception Island, Antarctica*. IEEE Transactions on Geoscience and Remote Sensing, **45** (1), 138–146.

Beyreuther M., Carniel R. and Wassermann J.; 2008: *Continuous hidden Markov Models: application to automatic earthquake detection and classification at Las Cañadas caldera, Tenerife*. Journal of Volcanology and Geothermal Research, **176** (4), 513-518.

Burlini L., Vinciguerra S., Di Toro G., De Natale G. and Burg J.-P.; 2007: *Seismicity preceding volcanic eruptions: new experimental insights*. Geology, **35** (2), 183-186.

Colombero C. and Comina C.; 2014: *Geophysical characterization of an instable rock mass*. In: Alejano L., Perucho A., Olalla C. and Jiménez R. (Eds): *Rock Engineering and Rock Mechanics: Structures in and on Rock Masses*. Eurock 2014 proceeding papers, Vigo (Spain), Taylor & Francis Group, London, 978-1-138-00149-7,

Cortés G., Arambula R., Gutiérrez L., Benítez C., Ibáñez J., Lesage P., Álvarez I. and García L.; 2009: Evaluating robustness of a HMM-based classification system of volcanoseismic events at Colima and Popocatepetl volcanoes. Geoscience and Remote Sensing Symposium, 2009 IEEE International, IGARSS, **2**, 1012 pp.

Falsaperla S., Graziani S., Nunnari G. and Spampinato S.; 1996: *Automatic classification of volcanic earthquakes by using multi-layered neural networks*. Natural Hazards, 13 (3), 205-228.

Giacco F., Esposito A.M., Scarpetta S., Giudicepietro F. and Marinaro M.; 2009: *Support vector machines and MLP for automatic classification of seismic signals at Stromboli volcano*. In: Apolloni B., Bassis S. and Morabito F.C. (Eds.), WIRN, *Frontiers in Artificial Intelligence and Applications*, **204**, IOS Press, pp. 116-123.

Helmstetter A. and Garambois S.; 2010: *Seismic monitoring of Sechilienne rockslide (French Alps): Analysis of seismic signals and their correlation with rainfalls*. J. Geophys. Res., **115** (F3), F03016.

Lancellotta R., Gigli P. and Pepe C.; 1991: Relazione tecnica riguardante la caratterizzazione geologico-strutturale dell'ammasso roccioso e le condizioni di stabilità della rupe. *Private communication*.

Levy C., Jongmans D. and Baillet L.; 2011: *Analysis of seismic signals recorded on a prone-to-fall rock column (Vercors massif, French Alps)*. Geophys. J. Int., **186**, 296-310.

Lomax A., Virieux J., Volant P. and Berge C.; 2000: *Probabilistic earthquake location in 3D and layered models: Introduction of a Metropolis-Gibbs method and comparison with linear locations*. In: Thurber C.H. and Rabinowitz N. (Eds.): *Advances in Seismic Event Location*, Kluwer, Amsterdam, pp.101-134.

Lytle R.J., Dines K.A., Laine E.F. and Lager D.L.; 1978: *Electromagnetic Cross-Borehole Survey of a Site Proposed for an Urban Transit Station*. UCRL-52484, Lawrence Livermore Laboratory, University of California, 19 pp.

Masotti M., Falsaperla S., Langer H., Spampinato S. and Campanini R.; 2006: *Application of support vector machine to the classification of volcanic tremor at Etna, Italy*. Geophysical Research Letters, **33**.

Peterson J.E., Paulson B.N.P. and McEvilly T.V.; 1985: *Applications of Algebraic Reconstruction Techniques to Crosshole Seismic Data*. Geophysics, **50**, 1566-1580.

Scarpetta S., Giudicepietro F., Ezin E., Petrosino S., Del Pezzo E., Martini M. and Marinaro M.; 2005: *Automatic classification of seismic signals at Mt. Vesuvius volcano, Italy, using neural networks*. Bulletin of the Seismological Society of America, **95** (1), 185-196.

Spillmann T., Maurer H., Green A.G., Heincke B., Willenberg H. and Husen S.; 2007: *Microseismic investigation of an unstable mountain slope in the Swiss Alps*. J. Geophys. Res., **112**, B07301.

Um J. and Thurber C.; 1987: *A Fast Algorithm for Two-Point Seismic Ray Tracing*. Bull. Seismol. Soc. Am., **77**, 972-986.

48